Article

Interlaboratory Comparison of Hydrogen-Deuterium Exchange Mass Spectrometry Measurements of the Fab fragment of NISTmAb

Jeffrey W. Hudgens, Elyssia S. Gallagher, Ioannis Karageorgos, Kyle W Anderson, James J. Filliben, Richard Y-C Huang, Guodong Chen, George M. Bou-Assaf, Alfonso Espada, Michael J. Chalmers, Eduardo Harguindey, Hui-Min Zhang, Benjamin T. Walters, Jennifer Zhang, John D. Venable, Caitlin Steckler, Inhee Park, Ansgar Brock, Xiaojun Lu, Ratnesh K. Pandey, Arun Chandramohan, Ganesh S. Anand, Sasidhar N. Nirudodhi, Justin B. Sperry, Jason C. Rouse, James A. Carroll, Kasper D. Rand, Ulrike Leurs, David D Weis, Mohammed A. Al-Naqshabandi, Tyler S. Hageman, Daniel Deredge, Patrick L. Wintrode, Malvina Papanastasiou, John D. Lambris, Sheng Li, and Sarah Urata

Anal. Chem., **Just Accepted Manuscript** • DOI: 10.1021/acs.analchem.9b01100 • Publication Date (Web): 02 May 2019

	Weis, David; University of Kansas, Chemistry Al-Naqshabandi, Mohammed; University of Kansas, Chemistry; Soran University, Department of General Science Hageman, Tyler; University of Kansas, Department of Chemistry Deredge, Daniel; University of Maryland School of Pharmacy, Pharmaceutical Sciences Wintrode, Patrick; University of Maryland School of Pharmacy, Department of Pharmaceutical Sciences Papanastasiou, Malvina; University of Pennsylvania Perelman School of Medicine, Department of Pathology & Laboratory Medicine Lambris, John; University of Pennsylvania Perelman School of Medicine, Department of Pathology & Laboratory Medicine Li, Sheng; University of California San Diego, Urata, Sarah; University of California San Diego, Department of Medicine

Interlaboratory Comparison of Hydrogen-Deuterium Exchange Mass Spectrometry Measurements of the Fab fragment of NISTmAb.

Jeffrey W. Hudgens*[,†,‡], Elyssia S. Gallagher[†,‡,◊,‖], Ioannis Karageorgos[†,‡,◊], Kyle W. Anderson[†,‡,◊], James J. Filliben[¶], Richard Y.-C. Huang[♣], Guodong Chen[♣], George M. Bou-Assaf[⊥], Alfonso Espada[#], Michael J. Chalmers[×], Eduardo Harguindey[#], Hui-Min Zhang[§], Benjamin T. Walters[§], Jennifer Zhang[§], John Venable[≠], Caitlin Steckler[≠,⊗,Λ], Inhee Park[≠,∅], Ansgar Brock[≠], Xiaojun Lu[∀,∇], Ratnesh Pandey[∀,∃], Arun Chandramohan[€,κ], Ganesh Srinivasan Anand[€], Sasidhar N. Nirudodhi[ϕ], Justin B. Sperry[Δ], Jason C. Rouse[Γ], James A. Carroll[Δ], Kasper D. Rand[Θ], Ulrike Leurs[Θ,π], David D. Weis[γ], Mohammed A. Al-Naqshabandi[γ,Σ], Tyler S. Hageman[γ], Daniel Deredge[β], Patrick L. Wintrode[β], Malvina Papanastasiou[Π,Ψ], John D. Lambris[Π], Sheng Li[&], and Sarah Urata[&,ϖ]

[†] National Institute of Standards and Technology, Bioprocess Measurement Group, Biomolecular Measurements Division, Rockville, MD 20850, United States

[‡]Institute for Bioscience and Biotechnology Research, 9600 Gudelsky Drive, Rockville Maryland 20850, United States

[¶]National Institute of Standards and Technology, Statistical Engineering Division, Gaithersburg, Maryland 20899, United States

[♣]Bristol-Myers Squibb Company, Pharmaceutical Candidate Optimization, Research and Development, Princeton, New Jersey 08540, United States

[⊥] Biogen Inc., Analytical Development, 225 Binney Street, Cambridge, Massachusetts 02142, United States

[#]Centro de Investigación Lilly S.A., 28108-Alcobendas, Spain

[×]Lilly Research Laboratories, Eli Lilly and Company, Indianapolis, Indiana 46285, United States

[§]Genentech, Inc. Protein Analytical Chemistry, 1 DNA Way, South San Francisco, California 94080, United States

[≠]Genomics Institute of the Novartis Research Foundation, 10675 John Jay Hopkins Drive, San Diego, California 92121, United States

[⊗]Joint Center for Structural Genomics, La Jolla, California 92037, United States

[∀]MedImmune LLC, One MedImmune Way, Gaithersburg, Maryland 20878, United States

[€]National University of Singapore, Department of Biological Sciences, 14, Science Drive 4, Singapore 117543

[ϕ]Pfizer Inc., Vaccine R&D, 401 N Middletown Rd, Pearl River, New York 10965, United States

[Δ]Pfizer Inc., Analytical R&D, 700 Chesterfield Parkway West, Chesterfield, Missouri 63017, United States

[Γ]Pfizer Inc., Analytical R&D, 1 Burtt Road, Andover, Massachusetts 01810, United States

[Θ]University of Copenhagen, Department of Pharmacy, Universitetsparken 2, DK-2100 Copenhagen, Denmark

[γ]University of Kansas, Department of Chemistry, 1567 Irving Hill Road, Lawrence, Kansas 66045, United States

[Σ]Soran University, Department of General Science, Kawa Street, Soran, Kurdistan Region, Iraq

[β]University of Maryland, Baltimore, School of Pharmacy, Department of Pharmaceutical Sciences, 20 North Pine Street, Baltimore, Maryland 21201, United States

[Π]University of Pennsylvania, Department of Pathology & Laboratory Medicine, Perelman School of Medicine, 402 Stellar-Chance Labs, 422 Curie Boulevard, Philadelphia, Pennsylvania 19104, United States

[&]University of California, San Diego, Department of Medicine, 9500 Gilman Drive, La Jolla, California 92093, United States

KEYWORDS. hydrogen-deuterium exchange, interlaboratory comparison, mass spectrometry, peptide, precision, proteomics, reference material, repeatability, reproducibility.

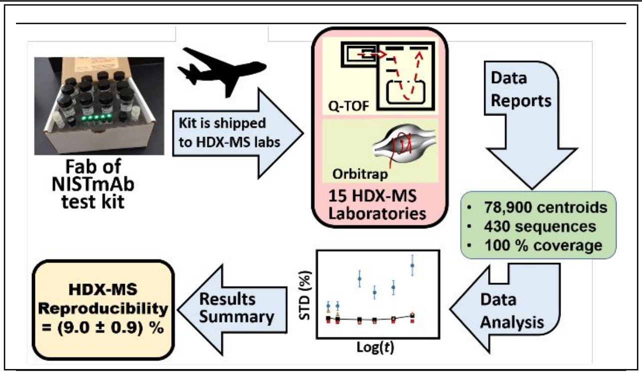

ABSTRACT: Hydrogen-deuterium exchange mass spectrometry (HDX-MS) is an established, powerful tool for investigating protein-ligand interactions, protein folding, and protein dynamics. However, HDX-MS is still an emergent tool for quality control of biopharmaceuticals and for establishing dynamic similarity between a biosimilar and an innovator therapeutic. Because industry will conduct quality control and similarity measurements over a product lifetime and in multiple locations, an understanding of HDX-MS reproducibility is critical. To determine the reproducibility of continuous-labeling, bottom-up HDX-MS measurements, the present interlaboratory comparison project evaluated deuterium uptake data from the Fab fragment of NISTmAb reference material (PDB: 5K8A) from fifteen laboratories. Laboratories reported ≈ 89,800 centroid measurements for 430 proteolytic peptide sequences of the Fab fragment (≈ 78,900 centroids), giving ≈ 100 % coverage, and ≈ 10,900 centroid measurements for 77 peptide sequences of the Fc fragment. Nearly half of peptide sequences are unique to the reporting laboratory, and only two sequences are reported by all laboratories. The majority of the laboratories (87 %) exhibited centroid mass laboratory repeatability precisions of $\langle s^{\mathrm{Lab}} \rangle \leq$ (0.15 ±0.01) Da ($1\sigma_{\bar{x}}$). All laboratories achieved $\langle s^{\mathrm{Lab}} \rangle \leq 0.4$ Da. For immersions of protein at T_{HDX} = (3.6 to 25) °C and for D_2O exchange times of t_{HDX} = (30 s to 4 h) the reproducibility of back-exchange corrected, deuterium uptake measurements for the 15 laboratories is $\sigma^{15\ \mathrm{Labs}}_{\mathrm{reproducibility}}(t_{\mathrm{HDX}})$ = (9.0 ±0.9) % (1σ). A 9 laboratory cohort that immersed samples at T_{HDX} = 25 °C exhibited reproducibility of $\sigma^{25\mathrm{C\ cohort}}_{\mathrm{reproducibility}}(t_{\mathrm{HDX}})$ = (6.5 ±0.6) % for back-exchange corrected, deuterium uptake measurements.

INTRODUCTION

Over the last twenty-eight years hydrogen-deuterium exchange mass spectrometry (HDX-MS) has developed into a powerful tool for investigating conformations, folding dynamics, and interactions among proteins including antibodies, glycoproteins, lipoproteins, membrane proteins, virus fragments, enzymes, chaperones, amyloids, fibrils, and pharmaceuticals. [1] The steady growth of HDX-MS studies is reflected in the 2247 original, heavily-cited research publications appearing through 2018 (Figure S1). [2] In the commercial sector HDX-MS data has been used to substantiate and protect intellectual property in >110 United States patents since 2010. [3] HDX-MS data are increasingly provided to support biologics license applications (BLAs). [4] During 2016, 15 % of BLAs to the FDA included HDX-MS data. [5] The increasing use of HDX-MS has been facilitated by rapid advances in the hardware and software that collect and analyze HDX-MS kinetics measurements. In short, HDX-MS has emerged from the "quicksand" of frontier science, [6] and it has become a mainstay tool in modern pharmaceutical [4, 7-26] and structural biology laboratories. [3, 23, 27-35]

Major advantages of HDX-MS for characterizing the conformational dynamics of proteins are its availability to make measurements under physiological conditions, its modest sample requirements, its use of proteomic informatics that link each HDX-MS peptide sequence directly to a portion of the subject protein, and its nearly unlimited capability to characterize large proteins, *e.g.*, antibodies (~150 kDa), [10, 12, 16, 19, 35] and viral capsids (~2 MDa). [36-42] The spatial structure obtained from X-ray and NMR structure analyses, cryogenic electron microscopy (cryo-EM), and the molecular dynamics revealed by HDX data can provide an improved description of the structure-function-dynamics relationships of a protein. [43]

HDX-MS is projected to have a role in quality control of biopharmaceuticals and for establishing dynamic similarity between a biosimilar and an innovator drug.[7, 10, 22, 44-45] As HDX-MS measurements are used to characterize materials that will enter commerce, customers may ask: How true and precise is the HDX-MS measurement?

Trueness is the nearness of agreement between the average of a large number of replicate measurements and a reference value. [46-47] Although numerous approaches to the prediction of H/D exchange rates coefficient are reported, [48-54] no means of accurately predicting exchange rates from first principles currently exist, and no reference materials with known exchange rates are available. Thus, we cannot easily establish the trueness of HDX-MS measurements. On the other hand, the precision metrics of HDX-MS can be evaluated because precision is just the closeness of agreement among measured values obtained by replicate measurements on the same or similar objects under specified conditions. [46] Precision is characterized by the components of repeatability, intermediate measurement precision (IMP), and reproducibility. [46] Determinations of reproducibility allow for variations of instruments, reagents, locations, and operators.

HDX-MS studies have reported daily repeatability ranging between 0.3 % to 2.9 % of maximum deuterium uptake and IMP's ranging between 1 % to 9 % over periods of 37 days to eight months.[7, 55-58] Cummins *et al.* compared

HDX-MS measurements for two laboratories harmonized by employing identical procedures and equipment. For ligand-vitamin D nuclear receptor complexes immersed 30 s in D_2O their results exhibited D-uptake repeatability and reproducibility of 0.54 % for a set of 35 peptide sequences.[59]

The objective of this study is to determine the reproducibility of continuous-labeling, bottom-up HDX-MS measurements (Figure 1). [60] Reproducibility is determined only through an interlaboratory comparison exercise that engages multiple laboratories in measurements of the same sample. [46] For the present unharmonized study investigators were permitted use of any HDX-MS instrumentation and software. The laboratories were not directed to report specific peptide sequences nor were they told the deuterium uptake rates of previously observed peptides. A determination of HDX-MS reproducibility will provide a measure of its present capability for evaluations of protein commercial products. Furthermore, an interlaboratory comparison project can itself stimulate improvements in measurement procedures and equipment.

EXPERIMENTAL METHODS

Bottom-up HDX-MS measurements. Laboratories conducted "bottom-up" HDX-MS experiments (Figure 1), using procedures known to provide excellent repeatability precision. [60-63] Immersion of Fab fragment of NISTmAb reference material (PDB: 5K8A) [64-66] sample in buffered solution (deuterium fraction, F^{D_2O} = 0.8 to 0.96) at temperature T_{HDX} and pD 7.48 induces D for H exchange (Figure 1A). At t_{HDX} the solution is diluted into an acidic solution (T_{quench} ≈ 0 °C, pH ≈ 2.5, F^{D_2O} = 0.18 to 0.48), containing chaotropic and reducing agents, [67] which denature the protein and reduce its disulfide bonds (Figure 1B). In this cold acidic solution,

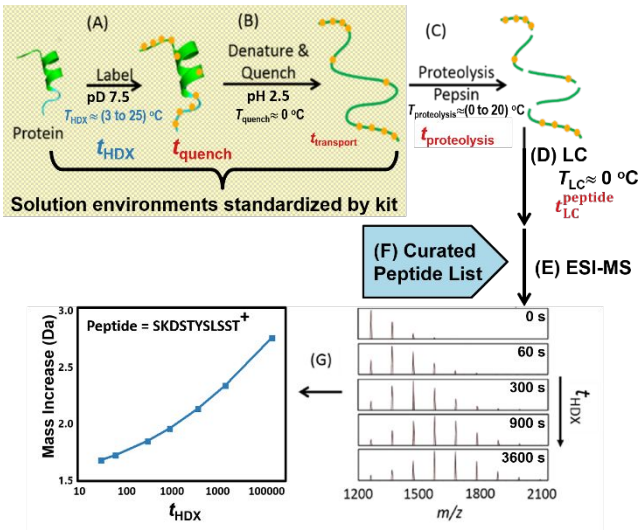

Figure 1. The "bottom-up" HDX-MS experiment broken into steps controlled by the NIST HDX-MS reagent kit (steps A and B in the yellow/gray box) and by each participating laboratory peptide (steps C through G). H for D back-exchange occurs during periods listed in red.

chemical exchange rates of amide sites in denatured proteins approach their minima. [68] All laboratories used the same HDX-MS kit (Figure S2) that provided buffers and reagents used during the first two steps (ref. yellow/gray box of Figure 1). The kit harmonized pH, salt concentration and reducing power (Table S1). However, specific requirements of laboratory apparatus (Tables S2 and S3) required adjustments to protein concentrations and F^{D_2O} (Table S5).

Subsequently, the denatured, quenched Fab solution passes into a column containing immobilized pepsin or pepsin/Protease from Aspergillus saitoi Type XIII blend (Figure 1C). [25, 69-70]. The protease digests the Fab fragment of NISTmAb ($\Delta t_{proteolysis}$ = (18 to 240) s, $T_{proteolysis}$ = (0 to 20) °C), and the effluent becomes trapped on a guard column (Figure 1D). By flowing additional solution through the guard column for t_{wash} = (30 to 180) s, many laboratories wash out salts. Reverse-phase chromatography, conducted at T_{LC} ≈ 0 °C, releases and separates peptides, which elute from the analytical column at $t_{LC}^{peptide}$ (Figure 1D). Electrospray ionization mass spectrometry (ESI-MS) detects the peptide ions (Figure 1E).

Alternately, immediately after D_2O incubation has completed (Figure 1B), some laboratories flash freeze the sample (Table S5). Subsequently, the sample is thawed and analyzed using a workflow similar to that depicted in Figures 2C through 2G.

The average mass change of each selected peptide (Figure 1F) is calculated and plotted as a function of t_{HDX} (Figure 1G). Since side chain amides generally exchange H/D more rapidly than backbone amides, [62, 68] the deuterium labels at these positions will have equilibrated during chromatography to the natural protic isotope abundance, thus, simplifying analyses.

Separate experiments, equivalent to the HDX-MS experiment for t_{HDX} = 0 s, determine the initial curated list of peptides (Figure 1F) that associates each chromatographic peak with mass spectra. To improve the veracity of peptide identifications, the operator observes MS/MS data for the eluting peptides. With reference to the known sequence of Fab of NISTmAb [65] peptide ion identification software (Tables S2 and S3) analyzes these data and proposes an amino acid sequence, charge state (z), and confidence rank for each peptide ion fragment. The list of retention times and sequences becomes the filter through which peptide ions are selected for HDX-MS analyses. Still, the curation process continues throughout the data analysis. Curation of the list ascertains that the exchange kinetics of sequences adhere to EX2 behavior, [1, 71-73] that the D-uptake kinetics match the sequence assignments, that the LC retention times remain stable, and that peptides exhibit adequate intensity to support reliable centroid determinations and remain free of interfering ion signals.

Each laboratory conducted proteomics studies on the Fab fragment of NISTmAb and performed three HDX–MS

runs. Each "run" comprises three replicant measurements, termed "reps", at each time point, t_{HDX}. Laboratories submitted spreadsheets of centroids and information about experimental conditions to a not-for-profit data service, NAPT (National Association for Proficiency Testing, Edina, MN), which anonymized the datasheets and forwarded them to the National Institute of Standards and Technology (NIST). The data are available for study. [74]

RESULTS

Laboratory Reports. The NIST Interlaboratory Comparison Project received fifteen anonymized datasets and associated documentation. The fifteen datasets contain ≈ 89,800 HDX-MS centroid measurements from 709 peptide ions, ranging from 456 m/z to 6048 m/z and $1 \le z \le 8$, comprising 507 unique amino acid sequences.

A few laboratories reported sequences of the Fc fraction of NISTmAb. These sequences were expected due to trace Fc present in the Fab stock solution. Since most of the laboratory cohort did not report Fc peptides, 100 Fc peptide ions (77 Fc sequences) were deleted from the working dataset. The reduced working dataset for the Fab protein comprises ≈ 78,900 centroids. The working dataset contains 609 peptide ions originating from 430 sequences of the light and heavy chains.

Laboratories reported the centroid mass $\langle m(t_{HDX})\rangle$, derived for each measurement at seven D_2O immersion times (Figure 1A), t_{HDX} = 0 s, 30 s, 60 s, 300 s, 900 s, 3,600 s, and 14,400 s. By measuring peptide ions observed from the finished Fab-D_2O sample, laboratories computed the centroid mass control value, $\langle m(\infty_{pseudo})\rangle$, corresponding to $t_{HDX} \approx \infty$ s.

Reference Peptide Maps. Colored stripes, Figure 2 illustrate the peptide ion sequences reported by all laboratories. With reference to the legend of Figure 2, the color of each stripe indicates its coincidence frequency (ω_i^c), which is the number of laboratories reporting the ith peptide sequence (ion of any z). The x-coordinates of each stripe correspond to the start and stop indices of the peptide sequence with reference to the Fab fragment of NISTmAb. The y-coordinate position of each strip allows a unique address for each sequence. The software drawing this map places the most frequently reported sequences (largest ω_i^c) at the lower ordinates. Where peptides of the same ω_i^c would overlap, one peptide is placed in the next higher vertical row.

Summation of all data for the Fab fragment yields a map of the heavy chain containing 221 peptide sequences (Figure 2A) and a map of the light chain containing 209 peptide sequences (Figure 2B). The sequences comprise between 4 and 60 amino acids. The set of 430 sequences reported by the laboratories has a median sequence length of 13 amino acids, and 84 % of the members in the set contain between 5 and 21 amino acids (Figure S3).

Although the laboratory cohort collectively reports sequences that cover the heavy and light chains comprehensively, most laboratories reported datasets holding lower sequence coverage. The peptide sequences reported by the laboratories number between 41 and 175, corresponding to coverages of 56 % to 99 % for the heavy chain and of 60 % to 99 % for the light chain (Figure S4).

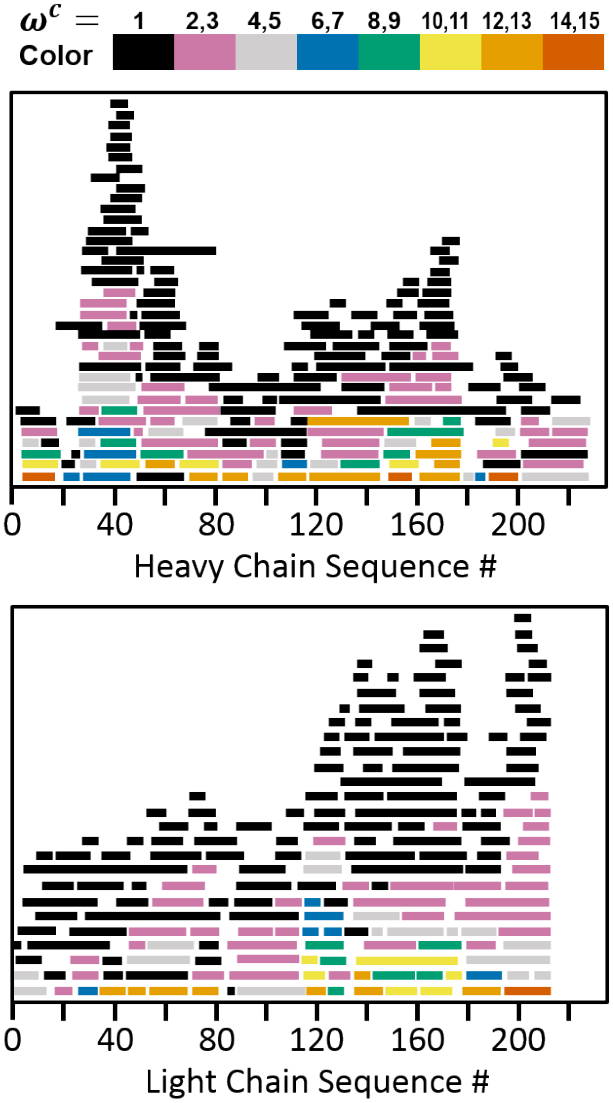

Figure 2. Reference peptide heat map of the peptide sequences reported by fifteen laboratories for Fab fragment of NISTmAb. Colors indicated on the legend denote the ω_i^c of each peptide sequence. Vertical placements of the sequence stripes are determined by sequence overlap and ω_i^c. Horizontal placements of stripes denote peptides between the N-terminal and C-terminal sequence indices for the: A) 221 sequences reported for the heavy chain, and B) 209 sequences reported for the light chain.

The sequence coincidence population, $M(\omega^c)$, is computed by counting the peptide sequences for each coincidence frequency, ω^c. For example, $M(1)$ = 245 (represented by black stripes in Figure 2) is the population of sequences listed once across all laboratory datasets. The population $M(1)$ of the Fab fragment comprises 48 % heavy chain sequences and 53 % light chain sequences. In Figure

2 stripes of other colors bars represent sequences listed twice or more across all laboratory datasets ($2 \le \omega_i^c \le 15$); thus, $\sum_2^{15} M(\omega^c)$ = 185 shared peptide sequences. (The working dataset is $\sum_1^{15} M(\omega^c)$ = 430.) Across the laboratory cohort, $M(\omega^c)$ falls rapidly with increasing coincidence frequency, such that only two peptide sequences are reported by all laboratories, i.e., $M(15) = 2$ (Figure S5).

The number of reported peptide sequences as a function of the six instrument-software configurations used by the laboratories was examined (Figure S6). On average, laboratories reported $\langle \overline{C} \rangle$ = 103 ± 41 (1σ) sequences. No laboratory reported peptide sequence populations falling outside the $\langle \overline{C} \rangle \pm 3\sigma$ boundaries that would identify outlying performance. This result suggests the each instrumentation-software configuration has nearly equal capacity to detect the numerous Fab fragments of NISTmAb emanating from its ESI source. Furthermore, we note that the use of a pepsin/Type XIII protease mixture by Lab 12 did not lead to identification of a superior, outlying number of peptides in comparison to the cohort using pepsin only.

Sensitivity Analyses of HDX-MS Measurements. Knowledge the overall effect of experimental factors will guide evaluation of the measurement uncertainty. One possible error could arise if the deuterium content of peptides varies as a function of charge. [75-76] Thus, deuterium content of centroids vs. peptide charge was examined for 513 peptides (z = +1 to +7) of 106 sequences reported by 13 laboratories. No evidence of systemic, in-ESI source, intermolecular H/D exchange was observed (Table S6).

Main effects plots reveal the overall effect of several experimental factors on the HDX-MS measurement. [77] The main effects of each independent variable on the $\%E_{\text{uncorrected}}$ and $\%E_{\text{corrected}}$ uptake measurements are found by averaging across the levels of the other independent variables of the HDX-MS experiment. For this study main effects are computed for the factors of t_{HDX}; *Lab*; $\%D_2O$; *Peptide*; T_{HDX}; *Rep#*, repetition number; *FROZEN*,

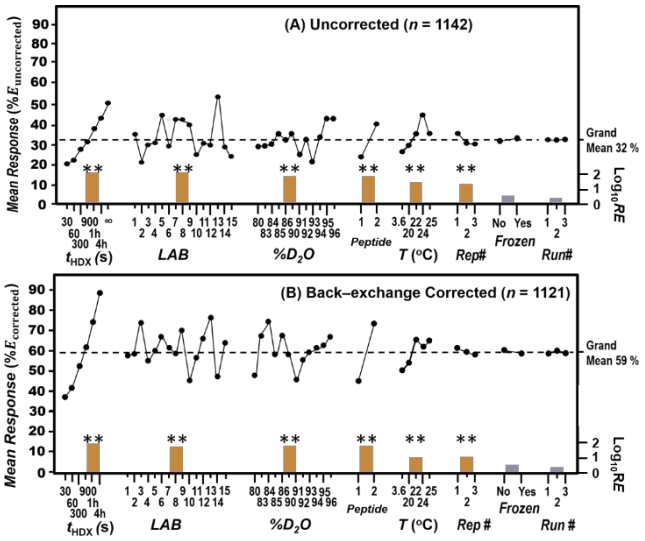

Figure 3. Main Effects Plots showing the variation of HDX-MS measurements for A) data uncorrected for back-exchange and B) data corrected for back-exchange. Bars denote $\log_{10}RE$ for each factor. Factors found by ANOVA to exert significant relative effect ($p < 0.01$) are marked with **. Dashed lines mark the mean deuterium uptake.

which is the flash-freezing of quenched sample prior to proteolysis; and *Run#*, run number. These computations used ≈ 1120 measurements reported by all laboratories for the two peptides: peptide 1, ^{149}VKDYFPEPVT^{158} of the heavy chain and peptide 2, ^{195}VTHQGLSSPVTKSFNRGEC^{213} of the light chain.

Figure 3A displays main effects for $\%E_{\text{uncorrected}}$, which are centroids processed with equation S3 and averaged from each variable. Figure 3B displays the main effects plots for $\%E_{\text{corrected}}$, which was computed with equation S5. On each panel a dashed line marks the *grand mean* of deuterium exchange, which is the average of data from all laboratories for both peptides. (We note that the correction for back-exchange increases the *grand mean* deuteration of the two peptides from 32 % to 59 %.) Factors are ranked from left to right in accord with decreasing relative effect (*RE*). Below each plot a colored bar shows the$\log_{10}RE$, which indicates the sensitivity for each factor. [77] To assess the statistical significance of the variance within the eight factors, analysis of variance (ANOVA) computations were carried out. [77-79] In Figure 3 factors exhibiting significant relative effect ($p < 0.01$) are marked with **.

As shown in Figure 3, some factors respond in good accord with the design of the HDX-MS experiment. As examples, *mean response* ($\%E_{\text{uncorrected}}$) rises from 18 % to 48 % between t_{HDX} = 30 s and $t_{\text{HDX}} = \infty_{\text{pseudo}}$, and peptides 1 and 2 exhibit different mean response, as expected for sequences residing in different local structural environments. Examination of the results for the procedure where samples are flash frozen (*FROZEN*= "yes") indicate that this procedure has little effect on precision. The *mean response* $\%E_{\text{uncorrected}}$ suggests a 1 % improvement in deuterium recovery; however, *mean response* $\%E_{\text{corrected}}$ reverses this effect by −2 %. Likewise, *mean response* ($\%E_{\text{uncorrected}}$) for *Run#* 1, 2, and 3 vary by

< 0.3 %, which provides assurance that day to day system performance is nearly invariant. These same trends are also observed in plots of $\%E_{\text{corrected}}$. ANOVA computations also confirm insignificant variances for factors *FROZEN* and *Run#*.

Main effects analyses reveal four non-ideal responses, and ANOVA verifies the significance of the variances. $\%E^{\text{peptide}}$ should not vary with factors of *Lab* or $\%D_2O$. Figure 3 shows that the *mean response* $\%E^{\text{peptide}}_{\text{uncorrected}}$ and *mean response* $\%E^{\text{peptide}}_{\text{corrected}}$ vary significantly for both factors. Moreover, the ideal HDX-MS experiment should exhibit null main effects with respect to *Rep#*; however, the *mean response* $\Delta(\%E_{\text{uncorrected}})$ exhibits a ≈ 3.5 % reduction between Rep 1 and Rep 3. After back-exchange correction the mean change remains $\Delta(\%E_{\text{corrected}})$ = 3.5 %. Since each series of reps is executed within the same run, the diminished response is likely a symptom of incomplete removal of peptides from the chromatographic apparatus between the replicate measurements. [80-81]

Temperature also affects acid and base catalyzed hydrogen-deuterium exchange rates. Amides undergo ≈ 3× increases in exchange rates for each increment of 10 °C. [82] In accord with this prediction, *mean response* of $\%E_{\text{corrected}}$

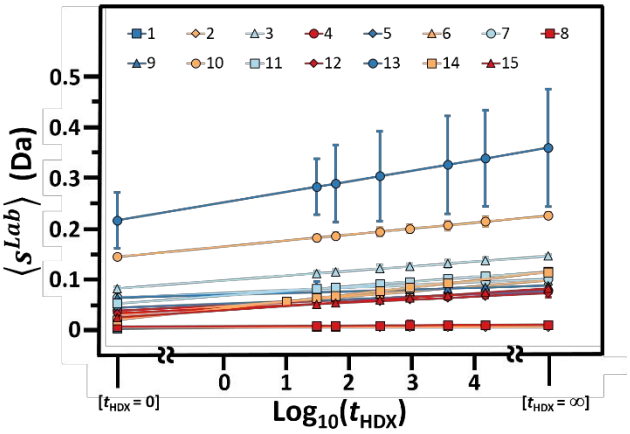

Figure 4. Repeatability plotted as average standard deviation $\langle s^{\text{Lab}} \rangle$ vs $\log_{10}(t_{\text{HDX}})$ for all peptide ions reported by each laboratory. When greater than the symbol, bars on each time point indicate one standard error of the mean, $\sigma_{\bar{x}}$.

(Figure 3B) increases as a function of T_{HDX} between 3.6 °C and 25 °C; however, some possible discordant response is displayed between 22 °C and 25 °C. Since the responses at 22 °C and 24 °C originate from two and one laboratories, respectively, it is difficult to separate effects of *Lab* and T_{HDX}. The main effects method does not reveal factors contributing to this incongruous response.

Determinations of Repeatability. Repeatability measurements provide insight into the *m/z* measurement stability of the sample handling, mass spectrometer, software, and procedures. Figure 4 presents the fits for $\langle s^{\text{Lab}} \rangle$ vs $\log_{10}(t_{\text{HDX}})$ for t_{HDX} = 0 s through $t_{\text{HDX}} = \infty_{\text{pseudo}}$ for each laboratory. The repeatability plot for each laboratory is constructed from a dataset comprising between 984 to 4057 $s^{Lab}_{\text{peptide}}(t_{\text{HDX}})$ values for 41 to 175 sequences in all reported charge states (Figure S7). Uncertainty bars on the $\langle s^{\text{Lab}} \rangle$ symbols indicate the standard error of the mean, $\sigma_{\bar{x}}$. For most laboratories $\sigma_{\bar{x}}$ < 0.007 Da, which corresponds to the size of the symbols in Figure 4. In summary, 87 % of laboratories exhibited centroid mass laboratory repeatability precisions of $\langle s^{Lab} \rangle \leq$ 0.15 Da, and the remaining 13 % have repeatability precisions characterized by 0.14 Da ≤ $\langle s^{\text{Lab}} \rangle$ ≤ 0.4 Da.

Reproducibility of HDX-MS. Reproducibility of HDX-MS is derived using sample standard deviations (equation S6) of $\%E^{\text{peptide}}_{\text{corrected}}$ for peptide sequences measured at the same T_{HDX}. The laboratories were divided into cohorts that measured $\%E^{\text{peptide}}_{\text{corrected}}$ at T_{HDX} = (25 ±1) °C, (21 ±1) °C, and (3.6 ±1) °C. Figure 5 shows plots of $\%E^{\text{peptide}}_{\text{corrected}}$ vs. $\log_{10}(t_{\text{HDX}})$ that were reported by the nine laboratories of the (25 ±1) °C cohort. Figure 6A plots the sample standard deviations as a function of $\log_{10}(t_{\text{HDX}})$ for peptides A-F (Figure 5) and peptides G-N (Figure S8). Each plot exhibits self-consistent D-uptake patterns. Figures 5D, S8G, S8L, and S8N exhibit D-uptake traces suggestive of kinetics that may be fit with multiple-exponential functions. [83] The weighted arithmetic mean of these standard deviations is $\sigma^{25\text{C cohort}}_{\text{reproducibility}}$ = (6.5 ±0.6) %. The nearly equal weighting of data from all laboratories (ωi^{c}= 8, 9) gives considerable statistical significance to this result.

The determination of $\sigma^{25\text{C cohort}}_{\text{reproducibility}}$ is also computed by expanding this analysis to include the complete subset of 130 sequences of $\omega i^{c} \geq 2$ and weighting each $s^{25\text{C cohort}}_{\text{sequence}}(t_{\text{HDX}})$ by the number of reporting laboratories. This computation yields $\sigma^{25\text{C cohort}}_{\text{reproducibility}}(t_{\text{HDX}})$ = (7.4 ±0.3) %. While robust, this value reflects skew from unequal weighting given by laboratories that have reported the most sequences. Reproducibility was also evaluated for $\omega i^{c} \geq 2$ sequences in other temperature cohorts (Figure 6b). Table 1 summarizes the determinations of $\sigma^{cohort}_{reproducibility}$ and the associated of the sample standard deviations of all temperatures is $\sigma^{15\text{ Labs}}_{\text{reproducibility}}(\text{t}_{\text{HDX}})$ = (9.0 ±0.9) %, where the weighting factors are a product of ωi^{c} and the number of sequences.

DISCUSSION

The NIST HDX-MS interlaboratory comparison project has found that 87 % of the laboratory cohort achieved a measurement repeatability precision of $\langle s^{\text{Lab}} \rangle \leq$ 0.15 ±0.01 Da ($1\sigma_{\bar{x}}$). All laboratories exhibited repeatability of $\langle s^{\text{Lab}} \rangle <$ 0.4 Da. The main effects analysis and measurements on

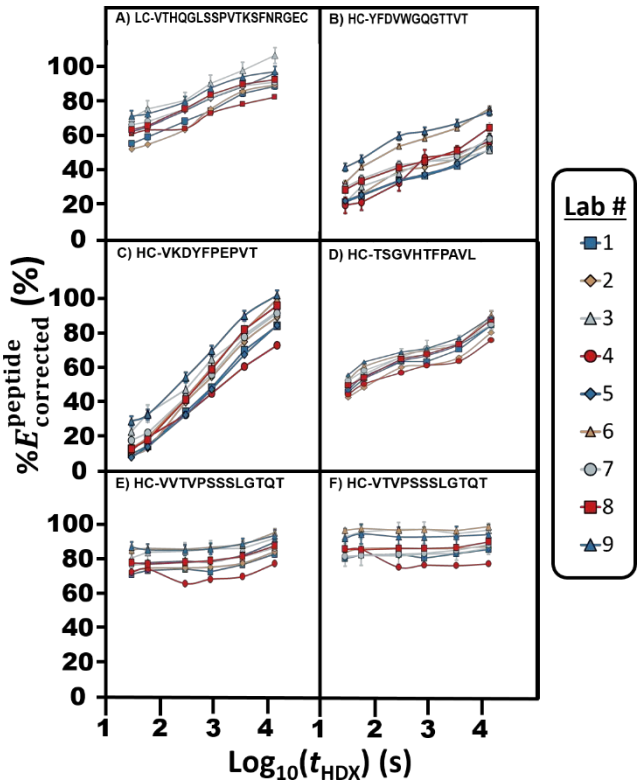

Figure 5. Plots of $\%E^{peptide}_{corrected}(t_{HDX})$ vs $\log_{10}(t_{HDX})$ for peptides measured at T_{HDX} = (25 ± 1) °C: A) LC-[195]VTHQGLSSPV-TKSFNRGEC[213], B) HC-[106]YFDVWGQGTTVT[117], C) HC-[149]VKDYFPEPVT[158], D) HC-[167]TSGVHTFPAVL[177], E) HC-[188]VVTVPSSSLGTQT[200], and F) HC-[189]VTVPSSSLGTQT[200]. Bars denote sample standard uncertainties larger than 1 %.

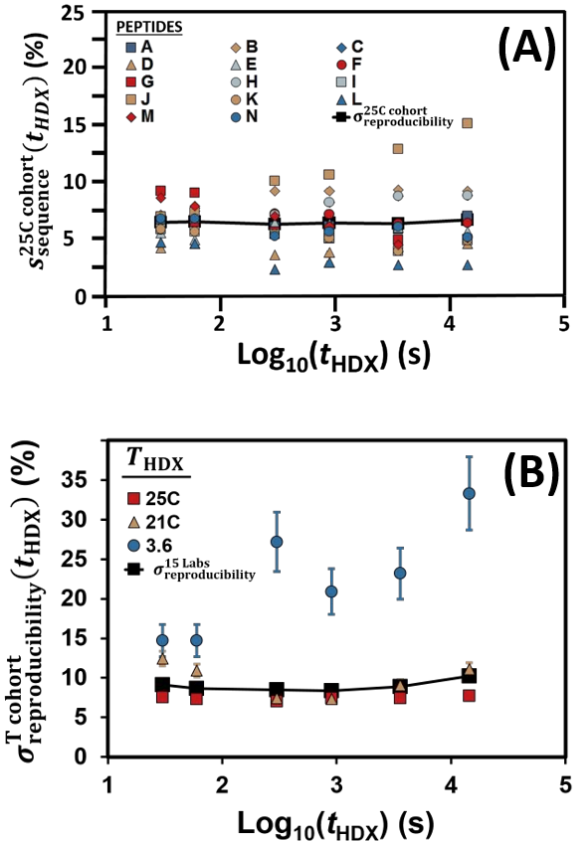

Figure 6. Determinations of HDX-MS reproducibility based on the sample standard deviation of $\%E^{peptide}_{corrected}$ for peptide sequences. A) $s^{25C\ cohort}_{sequence}(t_{HDX})$ (%) as a function of $\log_{10}(t_{HDX})$ for fourteen sequences measured at T_{HDX} = (25 ± 1) °C. Symbols denote the data from Peptides A-G (Figure 5) and Peptides H-N (Figure S8). Black squares and a trend line denote, $s^{25C\ cohort}_{reproducibility}(t_{HDX})$ (%) vs $\log_{10}(t_{HDX})$. Each black square is larger than the standard error of the mean, $\sigma_{\bar{x}} \approx 0.3$ %. B) $\sigma^{T\ cohort}_{reproducibility}(t_{HDX})$ (%) vs. $\log_{10}(t_{HDX})$ determined from $\%E^{peptide}_{corrected}$ for sequences measured at T_{HDX} = (25 ±1), (21 ±1), and (3.6 ±1) °C. Black squares and the trend line plot the weighted $\sigma^{15\ Labs}_{reproducibility}(t_{HDX})$ (%) as vs $\log_{10}(t_{HDX})$. Each black square is larger than its standard error of the mean, $\sigma_{\bar{x}} \leq 0.9$ %

Table 1. Summary of Reproducibility determinations for bottom-up HDX-MS for t_{HDX}= (30 to 14400) s.

T_{HDX}, °C	Lab cohort size	Number of sequences	ω_i^c	STD[a], %	$\sigma_{\bar{x}}^{wtd}$, %
25 ±1	9	14	8 to 9	6.5	0.6
25 ±1	9	130	2 to 9	7.4	0.3
21 ±1	4	88	2 to 4	9.7	0.7
3.6 ±1	2	26	2	22.3	3.1
Wtd Mean	15	244		9.0	0.9

a) $\sigma^{cohort}_{reproducibility}$

244 shared sequences have determined that the reproducibility of HDX-MS is $\langle\sigma^{\text{cohort}}_{\text{reproducibility}}\rangle$ = (9.0 ±0.9) %. Laboratories in the (25 ±1) °C cohort realized the reproducibility,

$\sigma^{25\text{C cohort}}_{\text{reproducibility}}$ = (6.5 ±0.6) %.

This analysis has used the correction for D_2O fraction and for back-exchange through measurements of $\langle m(0)\rangle^{\text{peptide}}$, $\langle m(t_{\text{HDX}})\rangle^{\text{peptide}}$, and $\langle m(\infty_{\text{pseudo}})\rangle^{\text{peptide}}$ on the same apparatus and with the same procedures (equation S5). [73, 84] The finishing procedure prescribed to prepare Fab-D_2O for measurements ensures that $\langle m(\infty_{\text{pseudo}})\rangle^{\text{peptide}}$ is essentially the same for all laboratories; thus, bias in the back-exchange calculation for each coincident peptide ($\omega^c_i \geq 2$) propagates equally across laboratories. Since such bias does not adversely affect the present determination of HDX-MS precision, the present results are suitable for computing the reproducibility of HDX-MS.

Intact protein mass spectrometry of Fab of NISTmAb reveals the possibility of nascent amide protons that are effectively unavailable for exchange (see Supporting Information), hence, $\langle m(\infty_{\text{pseudo}})\rangle^{\text{peptide}} < \langle m(\infty)\rangle^{\text{peptide}}$ for a fraction of the peptides. Consequently, the $\%E^{\text{peptide}}_{\text{corrected}}(t_{\text{HDX}})$ reported herein are not reference values for the Fab fragment of NISTmAb. The distribution of sequestered protons along the protein polymer is likely inhomogeneous, reflecting the most stable protein regions.

The main effects study reveals that the peptides reported by the cohort exhibit significant deuterium loss between the first and third chromatographic gradients (reps) conducted for a run. Since the loss of deuterium exchange is observed in $\%E^{\text{peptide}}_{\text{corrected}}$ and $\%E^{\text{peptide}}_{\text{uncorrected}}$ equally, the diminished response may evidence incomplete removal of peptides from the chromatographic apparatus between the replicate measurements. Adverse effects of carryover have been reported previously, and the magnitude of these effects can vary by peptide composition and column chemistry.[80-81] Diversity of the carryover contribution across laboratories increases the uncertainty of $\%E^{\text{peptide}}_{\text{corrected}}$. Thus, minimization of carryover is essential for accurate HDX-MS measurements.

The laboratory cohort reported peptide sequences with a coincidence frequency distribution containing 245 sequences of $\omega^c_i = 1$ and 185 sequences of coincidence frequencies of $2 \leq \omega^c_i \leq 15$ (Figure S5). In view of the diverse operating conditions of the protease columns (Tables S3 and S4), the importance of this result is uncertain.

Still, proteomics studies have reported that series of pepsin digests conducted under the same conditions display a great diversity of sequences and the prevalence of unique sequences ($\omega^c_i = 1$). [85-86] For example, Ahn *et al.* reported peptide identifications for a series of 31 digestions conducted at the same pH, salt concentration, temperature, and flow rate. [86] They found that a few (ubiquitous) peptides appeared in every digestion and that other peptides appeared only once in the digestion series. Unique peptic peptides outnumbered the reproducible peptides, and the number of unique peptides increased with each consecutive digestion. The number of reproducible peptides plateaued above 5 to 6 replicate digestions. In their study, a peptide was defined as "reproducible" when it appeared in 50 % of digestions.

The similar populations of $\omega^c_i = 1$ and $\omega^c_i > 1$ sequences and the rapid fall-off of coincidence population $M(\omega^c)$ to single digit coincidence frequency ω^c (Figure S5) suggest that the distribution of coincident sequences may follow a modified binomial function. [87] *In silico* digestion by pepsin of the light and heavy chains of Fab of NISTmAb generates a powerset of nearly 8100 peptide sequences containing 4 to 30 amino acids. (This calculation used the constraints that pepsin does not cleave at the P1 position for H, K, R, and P, nor at the P2 for P. [88]) When sample sizes are small compared to the total number of possible sequences, binomial functions predict that the number of unique sequences ($\omega^c_i = 1$) will be greater than the number of sequences of higher coincidence frequency ($\omega^c_i > 1$), as reported in this study. For the sample sizes reported by the laboratory cohort, most binomial models predict that no peptide sequence will manifest a coincidence frequency of $\omega^c_i > 6$.

Cleavage bias of pepsin and instrument fitness may also produce subset populations of ubiquitous sequences, δ_u, that exhibit sufficient signal to noise ratio (S/N)) for HDX-MS measurements by most laboratories. The ubiquitous sequences may account for the small set of peptide sequences with coincidence frequencies ranging $6 \leq \omega^c_i \leq 15$ (Figure S5). Thus, a modified binomial function may exist that can account for the $M(\omega^c)$ vs. ω^c distribution found for the laboratory cohort.

The plethora of peptic sequences produced from the Fab fragment may cause chromatographic crowding, confounding identifications. The surfeit of species may also result in ion suppression in the electrospray source of less abundant and difficult to ionize peptides. Dependent upon operating conditions and instrument fitness, peptides exhibiting marginal S/N may sporadically fall just within and just outside acceptance criteria for centroid determinations. For proteomics measurements of the same protein, each laboratory of the cohort may acquire a distinct subset of observed peptide sequences. Sequences within each subset may appear to be selected randomly from the powerset.

Inspection of Figure 2 shows that at least 32 sequences must be measured in order to describe 95 % of the Fab of NISTmAb HDX dynamics. For the quality control of a biotherapeutic product based solely on sequence-level comparisons of the deuterium content, the somewhat stochastic behavior of pepsin will add complexity, as not all sequences may be available during a measurement campaign. The quality control laboratory will usually observe the subset of ubiquitous sequences δ_u consistently, but the laboratory will likely need to repeat digestions until the necessary peptides are measured.

CONCLUSION

The NIST HDX-MS interlaboratory comparison project has analyzed fifteen HDX-MS datasets (≈ 78,900 centroids) for the Fab fragment of NISTmAb reference material. This study finds that most laboratories achieve a measurement repeatability precision of $\langle s^{\mathrm{Lab}} \rangle \leq 0.15 \pm 0.01$ Da ($1\sigma_{\bar{x}}$). Plots of repeatability can help assess HDX-MS system fitness and reveal procedural problems. Bottom-up HDX-MS generally has a reproducibility of $\langle \sigma^{\mathrm{cohort}}_{\mathrm{reproducibility}} \rangle = (9.0 \pm 0.9)$ %. The distribution of peptic peptides reported by the laboratory cohort exhibit relatively few coincidences. This low coincidence frequency distribution may require quality control methods based on bottom-up HDX-MS to perform repeated measurements to acquire a suitable number of peptides.

ASSOCIATED CONTENT

The Supporting Information is available free of charge on the ACS Publications website at DOI: XXXXXXXX

Descriptions of materials, metrological methods, computational methods, and supplementary results. Figures of HDX-MS publications and citations vs publication year, histogram of peptide sequence lengths, sequence coverage maps, performance of instrument-software configurations, repeatability plots, $\%E^{peptide}_{corrected}$ (t_{HDX}) vs $\log_{10}(t_{\mathrm{HDX}})$ for eight peptides. Tables of instrumentation, software, peptide search methodology, and operating conditions of proteolytic, chromatographic components, and effects of peptide charge on deuterium uptake. (PDF)

AUTHOR INFORMATION

Corresponding Author

*jeffrey.hudgens@nist.gov

ORCID

Ansgar Brock: 0000-0002-8080-3107
Arun Chandramohan: 0000-0002-4175-5886
Guodong Chen: 0000-0002-5531-407X
Daniel Deredge: 0000-0002-6897-6523
Alfonso Espada: 0000-0002-8301-1201
Eduardo Harguindey: 0000-0002-9291-0591
Ioannis Karageorgos: 0000-0002-2799-766X
Ulrike Leurs: 0000-0002-8828-3505
Sheng Li: 0000-0002-9073-6809
Xiaojun Lu: 0000-0001-5251-4343
Ratnesh Pandey: 0000-0002-0072-6480
Malvina Papanastasiou: 0000-0003-3378-6612
Inhee Park: 0000-0001-9161-438X
Ganesh Srinivasan Anand: 0000-0001-8995-3067
Caitlin Steckler: 0000-0001-5400-0696
Sarah Urata: 0000-0001-7512-4081
John Venable: 0000-0002-9938-4643
Hui-Min Zhang: 0000-0002-2099-4730
Jennifer Zhang: 0000-0002-9036-0477
Mohammed A. Al-Naqshabandi: 0000-0003-0839-5636
Kyle W. Anderson: 0000-0002-2808-3026
George M. Bou-Assaf: 0000-0003-4285-5915
James A. Carroll: 0000-0001-6790-0087
Michael J. Chalmers: 0000-0002-2139-6089
James J. Filliben: 0000-0002-2388-3198
Elyssia S. Gallagher: 0000-0002-5411-7285
Tyler S. Hageman: 0000-0003-0112-8893
Richard Y.-C. Huang: 0000-0002-7172-110X
Jeffrey W. Hudgens: 0000-0003-2805-1048
John D. Lambris: 0000-0002-9370-5776
Sasidhar N. Nirudodhi: 0000-0002-1827-7177
Kasper D. Rand: 0000-0002-6337-5489
Jason C. Rouse: 0000-0002-2721-7264
Justin B. Sperry: 0000-0002-3274-2194
Benjamin T. Walters: 0000-0001-5400-0696
David D. Weis: 0000-0003-3032-1211
Patrick L. Wintrode: 0000-0003-1866-9397

Present Addresses

[‖]Baylor University, Department of Chemistry and Biochemistry, One Bear Place #97348, Waco, TX, 76798, United States; Email: Elyssia_Gallagher@baylor.edu
[^]The Rockefeller University, Proteomics Resource Center, 1230 York Avenue New York, NY 10065-6399, United States. Email: Caitlin.Steckler@Rockefeller.edu
[∅]Computer Science, San Jose State University, San Jose, CA 95192; Email: inhee.park@sjsu.edu
[▽]Adimab LLC, 7 Lucent Dr, Lebanon, NH 03766; email: lxj_cwru@yahoo.com
[∃]GSK Vaccines, 14200 Shady Grove Road, Rockville, MD 20850; Email: ratnesh.k.pandey@gsk.com
[ϰ]Merck Sharp & Dohme Corp., 50 Tuas West Dr, Singapore 638408; Email: arun.chandramohan@merck.com
[π]Blegdamsvej 3B, Mærsk Tower floor 9, Department of Biomedical Sciences, Faculty of Health and Medical Sciences, University of Copenhagen, Denmark; Email: ulrike.leurs@sund.ku.dk
[Ψ]Broad Institute of MIT & Harvard, 415 Main St, Cambridge, MA 02142; Email: malpap@broadinstitute.org
[ϖ]Email: sarah.urata@gmail.com

Author Contributions

[◊]These authors contributed equally. The manuscript was written through contributions of all authors. All authors have given approval to the final version of the manuscript.

Funding Sources

The NIST project (design, test reagents, data analysis, and manuscript preparation) was funded by the NIST Biomanfacturing Program, and the project design precludes

the presence of competing financial interests. CS was supported by the National Institute of General Medical Sciences of the National Institutes of Health (NIH), Award Number **U54 GM094586**. GSA was supported by grants from the Singapore Ministry of Education Academic Research Fund Tier 3 (No. **MOE2012-T3-1-008**). KDR acknowledges financial support from the Danish Council for Independent Research (**Sapere Aude Grant-DFF-4184-00537A**). DD and PW declare that work at their institution was supported in part by the University of Maryland Baltimore, School of Pharmacy Mass Spectrometry Center (**SOP1841-IQB2014**). MP and JDL declare that work conducted at their institution was supported by National Institutes of Health (grants **AI068730** and **AI030040**).

Disclaimer

Certain commercial materials and equipment are identified in order to adequately specify experimental procedures. Such identifications neither imply recommendation or endorsement by the National Institute of Standards and Technology nor does it imply that the material or equipment identified is the best available for the purpose.

ACKNOWLEDGMENTS

JWH at NIST wishes to acknowledge Dr. Dean Ripple for his advice on procedures and legal hurdles, Dr. Andrew L. Rukhin for discussions on probability problems, Ms. Tsega Solomon for her assistance with experiments, and Ms. Natalie McDonald for assistance with the composition analysis software and data archival. JWH also thanks Dr. Yoshitomo Hamuro for insightful discussions. IK, ESG, and KWA of NIST and IBBR acknowledge support from the NIST National Research Council (NRC) Postdoctoral Research Associateship Program. RYCH and GC of Bristol-Myers Squibb acknowledge Dr. Adrienne Tymiak and Dr. Bruce Car for their support of this project. AE and EH at Centro de Investigación Lilly, S.A. acknowledge Mr. Sergio Cano for technical assistance. HMZ, BW, and JZ at Genentech, Inc. acknowledge Dr. Yung-Hsiang Kao and Dr. John Stults for their support for this project. XL and RP of MedImmune LLC acknowledge Dr. Qing (Paula) Lei and Dr. Michael Washabaugh for their support for this study. DDW at University of Kansas acknowledges Agilent Technologies for an equipment loan.

REFERENCES

1. Weis, D. D., *Hydrogen Exchange Mass Spectrometry of Proteins: Fundamentals, Methods, and Applications*. 1st Ed. ed.; John Wiley & Sons, Ltd.: Chichester, 2016.
2. Web of Science Database Search on HDX-MS of proteins and peptides (no reviews or commentary). Clarivate Analytics: Philadelphia, PA, 2019; (accessed 18 FEB 2019).
3. Google Patents. Alphabet Corp.: 2017; (accessed 9/25/2017).
4. Rogstad, S.; Faustino, A.; Ruth, A.; Keire, D.; Boyne, M.; Park, J., A Retrospective Evaluation of the Use of Mass Spectrometry in FDA Biologics License Applications. *J. Am. Soc. Mass Spectrom.* **2017,** *28* (5), 786-794.
5. Gutierrez-Lugo, M., Regulatory Consideration for the Characterization of HOS in Biotechnology Products. In *HOS 2016*, Olson, R., Ed. CASSS: Long Beach, CA, 2016.
6. Iacob, R. E.; Engen, J. R., Hydrogen Exchange Mass Spectrometry: Are We Out of the Quicksand? *J. Am. Soc. Mass Spectrom.* **2012,** *23* (6), 1003-1010.
7. Houde, D.; Berkowitz, S. A.; Engen, J. R., The Utility of Hydrogen/Deuterium Exchange Mass Spectrometry in Biopharmaceutical Comparability Studies. *J. Pharm. Sci.* **2011,** *100* (6), 2071-2086.
8. Berkowitz, S. A.; Engen, J. R.; Mazzeo, J. R.; Jones, G. B., Analytical tools for characterizing biopharmaceuticals and the implications for biosimilars. *Nature Reviews Drug Discovery* **2012,** *11* (7), 527-540.
9. Wei, H.; Ahn, J.; Yu, Y. Q.; Tymiak, A.; Engen, J. R.; Chen, G., Using Hydrogen/Deuterium Exchange Mass Spectrometry to Study Conformational Changes in Granulocyte Colony Stimulating Factor upon PEGylation. *J. Am. Soc. Mass Spectrom.* **2012,** *23* (3), 498-504.
10. Visser, J.; Feuerstein, I.; Stangler, T.; Schmiederer, T.; Fritsch, C.; Schiestl, M., Physicochemical and Functional Comparability Between the Proposed Biosimilar Rituximab GP2013 and Originator Rituximab. *Biodrugs* **2013,** *27* (5), 495-507.
11. Iacob, R. E.; Chen, G.; Ahn, J.; Houel, S.; Wei, H.; Mo, J.; Tao, L.; Cohen, D.; Xie, D.; Lin, Z.; Morin, P. E.; Doyle, M. L.; Tymiak, A. A.; Engen, J. R., The influence of adnectin binding on the extracellular domain of epidermal growth factor receptor. *J. Am. Soc. Mass Spectrom.* **2014,** *25* (12), 2093-2102.
12. Beck, A.; Debaene, F.; Diemer, H.; Wagner-Rousset, E.; Colas, O.; Van Dorsselaer, A.; Cianferani, S., Cutting-edge mass spectrometry characterization of originator, biosimilar and biobetter antibodies. *Journal of Mass Spectrometry* **2015,** *50* (2), 285-297.
13. Pan, J.; Borchers, C. H., Top-down mass spectrometry and hydrogen/deuterium exchange for comprehensive structural characterization of interferons: Implications for biosimilars. *Proteomics* **2014,** *14* (10), 1249-1258.
14. Leurs, U.; Mistarz, U. H.; Rand, K. D., Getting to the core of protein pharmaceuticals--Comprehensive structure analysis by mass spectrometry. *Eur J Pharm Biopharm* **2015,** *93*, 95-109.
15. Campobasso, N.; Huddler, D., Hydrogen deuterium mass spectrometry in drug discovery. *Bioorganic & Medicinal Chemistry Letters* **2015,** *25* (18), 3771-3776.
16. Majumdar, R.; Esfandiary, R.; Bishop, S. M.; Samra, H. S.; Middaugh, C. R.; Volkin, D. B.; Weis, D. D., Correlations between changes in conformational dynamics and physical stability in a mutant IgG1 mAb engineered for extended serum half-life. *mAbs* **2015,** *7* (1), 84-95.
17. Iacob, R. E.; Krystek, S. R.; Huang, R. Y. C.; Wei, H.; Tao, L.; Lin, Z.; Morin, P. E.; Doyle, M. L.; Tymiak, A. A.; Engen, J. R.; Chen, G., Hydrogen/Deuterium Exchange Mass Spectrometry Applied to IL-23 Interaction Characteristics: Potential Impact for Therapeutics. *Expert review of proteomics* **2015,** *12* (2), 159-169.
18. Deng, B.; Lento, C.; Wilson, D. J., Hydrogen deuterium exchange mass spectrometry in biopharmaceutical discovery and development - A review. *Analytica Chimica Acta* **2016,** *940*, 8-20.
19. Pan, J.; Zhang, S.; Chou, A.; Borchers, C. H., Higher-order structural interrogation of antibodies using middle-down hydrogen/deuterium exchange mass spectrometry. *Chemical Science* **2016,** *7* (2), 1480-1486.
20. Nazari, Z. E.; van de Weert, M.; Bou-Assaf, G.; Houde, D.; Weiskopf, A.; Rand, K. D., Rapid Conformational Analysis of Protein Drugs in Formulation by Hydrogen/Deuterium Exchange Mass Spectrometry. *J. Pharm. Sci.* **2016,** *105* (11), 3269-3277.
21. Iacob, R. E.; Engen, J. R.; Krull, I. S.; Rathore, A., Applicability of Hydrogen-Deuterium Exchange in Comparing Conformations of Innovator to Biosimilar Biopharmaceutical Products. *Lc Gc North America* **2017,** *35* (6), 382-390.

22. Masson, G. R.; Jenkins, M. L.; Burke, J. E., An overview of hydrogen deuterium exchange mass spectrometry (HDX-MS) in drug discovery. *Expert Opinion on Drug Discovery* **2017,** *12* (10), 981-994.

23. Huang, R. Y. C.; Iacob, R. E.; Krystek, S. R.; Jin, M.; Wei, H.; Tao, L.; Das, T. K.; Tymiak, A. A.; Engen, J. R.; Chen, G. D., Characterization of Aggregation Propensity of a Human Fc-Fusion Protein Therapeutic by Hydrogen/Deuterium Exchange Mass Spectrometry. *J. Am. Soc. Mass Spectrom.* **2017,** *28* (5), 795-802.

24. Huang, R. Y.-C.; Chen, G., Higher order structure characterization of protein therapeutics by hydrogen/deuterium exchange mass spectrometry. *Analytical and Bioanalytical Chemistry* **2014,** *406* (26), 6541-6558.

25. Nirudodhi, S. N.; Sperry, J. B.; Rouse, J. C.; Carroll, J. A., Application of Dual Protease Column for HDX-MS Analysis of Monoclonal Antibodies. *J. Pharm. Sci.* **2017,** *106* (2), 530-536.

26. Huang, R. Y. C.; Krystek, S. R.; Felix, N.; Graziano, R. F.; Srinivasan, M.; Pashine, A.; Chen, G., Hydrogen/deuterium exchange mass spectrometry and computational modeling reveal a discontinuous epitope of an antibody/TL1A Interaction. *mAbs* **2018,** *10* (1), 95-103.

27. Englander, S. W., Protein folding intermediates and pathways studied by hydrogen exchange. *Annual Review of Biophysics and Biomolecular Structure* **2000,** *29*, 213-238.

28. Hoofnagle, A. N.; Resing, K. A.; Ahn, N. G., Protein analysis by hydrogen exchange mass spectrometry. *Annual Review of Biophysics and Biomolecular Structure* **2003,** *32*, 1-25.

29. Lu, X. J.; Wintrode, P. L.; Surewicz, W. K., beta-Sheet core of human prion protein amyloid fibrils as determined by hydrogen/deuterium exchange. *Proceedings of the National Academy of Sciences of the United States of America* **2007,** *104* (5), 1510-1515.

30. Konermann, L.; Pan, J. X.; Liu, Y. H., Hydrogen exchange mass spectrometry for studying protein structure and dynamics. *Chemical Society Reviews* **2011,** *40* (3), 1224-1234.

31. Engen, J. R.; Wales, T. E.; Chen, S. G.; Marzluff, E. M.; Hassell, K. M.; Weis, D. D.; Smithgall, T. E., Partial cooperative unfolding in proteins as observed by hydrogen exchange mass spectrometry. *International Reviews in Physical Chemistry* **2013,** *32* (1), 96-127.

32. Shukla, A. K.; Westfield, G. H.; Xiao, K. H.; Reis, R. I.; Huang, L. Y.; Tripathi-Shukla, P.; Qian, J.; Li, S.; Blanc, A.; Oleskie, A. N.; Dosey, A. M.; Su, M.; Liang, C. R.; Gu, L. L.; Shan, J. M.; Chen, X.; Hanna, R.; Choi, M. J.; Yao, X. J.; Klink, B. U.; Kahsai, A. W.; Sidhu, S. S.; Koide, S.; Penczek, P. A.; Kossiakoff, A. A.; Woods, V. L.; Kobilka, B. K.; Skiniotis, G.; Lefkowitz, R. J., Visualization of arrestin recruitment by a G-protein-coupled receptor. *Nature* **2014,** *512* (7513), 218-+.

33. Englander, S. W.; Mayne, L.; Kan, Z. Y.; Hu, W. B., Protein Folding-How and Why: By Hydrogen Exchange, Fragment Separation, and Mass Spectrometry. In *Annual Review of Biophysics, Vol 45*, Dill, K. A., Ed. 2016; Vol. 45, pp 135-152.

34. Adhikary, S.; Deredge, D. J.; Nagarajan, A.; Forrest, L. R.; Wintrode, P. L.; Singh, S. K., Conformational dynamics of a neurotransmitter:sodium symporter in a lipid bilayer. *Proceedings of the National Academy of Sciences* **2017,** *114* (10), E1786-E1795.

35. Papanastasiou, M.; Koutsogiannaki, S.; Sarigiannis, Y.; Geisbrecht, B. V.; Ricklin, D.; Lambris, J. D., Structural Implications for the Formation and Function of the Complement Effector Protein iC3b. *The Journal of Immunology* **2017,** *198* (8), 3326-3335.

36. Pirrone, G. F.; Iacob, R. E.; Engen, J. R., Applications of Hydrogen/Deuterium Exchange MS from 2012 to 2014. *Anal. Chem.* **2015,** *87* (1), 99-118.

37. Bereszczak, J. Z.; Rose, R. J.; van Duijn, E.; Watts, N. R.; Wingfield, P. T.; Steven, A. C.; Heck, A. J. R., Epitope-distal Effects Accompany the Binding of Two Distinct Antibodies to Hepatitis B Virus Capsids. *Journal of the American Chemical Society* **2013,** *135* (17), 6504-6512.

38. Bereszczak, J. Z.; Watts, N. R.; Wingfield, P. T.; Steven, A. C.; Heck, A. J. R., Assessment of differences in the conformational flexibility of hepatitis B virus core-antigen and e-antigen by hydrogen deuterium exchange-mass spectrometry. *Protein Science* **2014,** *23* (7), 884-896.

39. Snijder, J.; Benevento, M.; Moyer, C. L.; Reddy, V.; Nemerow, G. R.; Heck, A. J. R., The Cleaved N-Terminus of pVI Binds Peripentonal Hexons in Mature Adenovirus. *Journal of Molecular Biology* **2014,** *426* (9), 1971-1979.

40. Wijesinghe, K. J.; Urata, S.; Bhattarai, N.; Kooijman, E. E.; Gerstman, B. S.; Chapagain, P. P.; Li, S.; Stahelin, R. V., Detection of lipid-induced structural changes of the Marburg virus matrix protein VP40 using hydrogen/deuterium exchange-mass spectrometry. *Journal of Biological Chemistry* **2017,** *292* (15), 6108-6122.

41. Johnson, B.; Li, J.; Adhikari, J.; Edwards, M. R.; Zhang, H.; Schwarz, T.; Leung, D. W.; Basler, C. F.; Gross, M. L.; Amarasinghe, G. K., Dimerization Controls Marburg Virus VP24-dependent Modulation of Host Antioxidative Stress Responses. *Journal of Molecular Biology* **2016,** *428* (17), 3483-3494.

42. Lim, X. X.; Chandramohan, A.; Lim, X. Y. E.; Bag, N.; Sharma, K. K.; Wirawan, M.; Wohland, T.; Lok, S. M.; Anand, G. S., Conformational changes in intact dengue virus reveal serotype-specific expansion. *Nature Communications* **2017,** *8*.

43. Noble, A. J.; Zhang, Q.; O'Donnell, J.; Hariri, H.; Bhattacharya, N.; Marshall, A. G.; Stagg, S. M., A pseudoatomic model of the COPII cage obtained from cryo-electron microscopy and mass spectrometry. **2012,** *20* (2), 167-173.

44. Marriott , J.; O'Connor, G.; Parkes, H. Study of Measurement Service and Comparison Needs for an International Measurement Infrastructure for the Biosciences and Biotechnology: Input for the BIPM Work Programme http://www.bipm.org/utils/common/pdf/rapportBIPM/2011/02.pdf (accessed 6-9-2018).

45. Wei, H.; Mo, J. J.; Tao, L.; Russell, R. J.; Tymiak, A. A.; Chen, G. D.; Iacob, R. E.; Engen, J. R., Hydrogen/deuterium exchange mass spectrometry for probing higher order structure of protein therapeutics: methodology and applications. *Drug Discov. Today* **2014,** *19* (1), 95-102.

46. JGCM 200 2012 International vocabulary of metrology – Basic and general concepts and associated terms (VIM) Joint Committee for Guides in Metrology 2012. (2008 edn with minor corrections) ed.; Bureau International des Poids et Mesures: Cedex, France, 2012. http://www.bipm.org/en/publications/guides/vim.html.

47. Menditto, A.; Patriarca, M.; Magnusson, B., Understanding the meaning of accuracy, trueness and precision. *Accred Qual Assur* **2007,** *12* (1), 45-47.

48. Petruk, A. A.; Defelipe, L. A.; Rodríguez Limardo, R. G.; Bucci, H.; Marti, M. A.; Turjanski, A. G., Molecular Dynamics Simulations Provide Atomistic Insight into Hydrogen Exchange Mass Spectrometry Experiments. *Journal of Chemical Theory and Computation* **2013,** *9* (1), 658-669.

49. McAllister, R. G.; Konermann, L., Challenges in the Interpretation of Protein H/D Exchange Data: A Molecular Dynamics Simulation Perspective. *Biochemistry* **2015,** *54* (16), 2683-2692.

50. Borysik, A. J., Simulated Isotope Exchange Patterns Enable Protein Structure Determination. *Angewandte Chemie International Edition* **2017,** *56* (32), 9396-9399.

51. Mazur, S. J.; Gallagher, E. S.; Debnath, S.; Durell, S. R.; Anderson, K. W.; Jenkins, L. M. M.; Appella, E.; Hudgens, J. W., Conformational Changes in Active and Inactive States of Human PP2C alpha Characterized by Hydrogen/Deuterium Exchange-Mass Spectrometry. *Biochemistry* **2017,** *56* (21), 2676-2689.

52. Boon, P. L. S.; Saw, W. G.; Lim, X. X.; Raghuvamsi, P. V.; Huber, R. G.; Marzinek, J. K.; Holdbrook, D. A.; Anand, G. S.; Grüber, G.; Bond, P. J., Partial Intrinsic Disorder Governs the Dengue Capsid Protein Conformational Ensemble. *ACS Chemical Biology* **2018,** *13* (6), 1621-1630.

53. Mohammadiarani, H.; Shaw, V. S.; Neubig, R. R.; Vashisth, H., Interpreting Hydrogen–Deuterium Exchange Events in Proteins Using Atomistic Simulations: Case Studies on Regulators of G-Protein Signaling Proteins. *The Journal of Physical Chemistry B* **2018,** *122* (40), 9314-9323.

54. Markwick, P. R. L.; Peacock, R. B.; Komives, E. A., Accurate Prediction of Amide Exchange in the Fast Limit Reveals Thrombin Allostery. *Biophysical Journal* **2019,** *116* (1), 49-56.

55. Chalmers, M. J.; Busby, S. A.; Pascal, B. D.; He, Y.; Hendrickson, C. L.; Marshall, A. G.; Griffin, P. R., Probing Protein Ligand Interactions by Automated Hydrogen/Deuterium Exchange Mass Spectrometry. *Anal. Chem.* **2006,** *78* (4), 1005-1014.

56. Burkitt, W.; O'Connor, G., Assessment of the repeatability and reproducibility of hydrogen/deuterium exchange mass spectrometry measurements. *Rapid Commun. Mass Spectrom.* **2008,** *22* (23), 3893-3901.

57. Chalmers, M. J.; Pascal, B. D.; Willis, S.; Zhang, J.; Iturria, S. J.; Dodge, J. A.; Griffin, P. R., Methods for the analysis of high precision differential hydrogen–deuterium exchange data. *International Journal of Mass Spectrometry* **2011,** *302* (1–3), 59-68.

58. Hudgens, J. W.; Huang, R. Y.-C.; D'Ambro, E., Method Validation and Standards in Hydrogen Exchange Mass Spectrometry In *Hydrogen Exchange Mass Spectrometry of Proteins: Fundamentals, Methods, and Applications*, 1st ed.; Weis, D. D., Ed. John Wiley & Sons, Ltd.: Chichester, 2016; pp 55-72.

59. Cummins, D. J.; Espada, A.; Novick, S. J.; Molina-Martin, M.; Stites, R. E.; Espinosa, J. F.; Broughton, H.; Goswami, D.; Pascal, B. D.; Dodge, J. A.; Chalmers, M. J.; Griffin, P. R., Two-Site Evaluation of the Repeatability and Precision of an Automated Dual-Column Hydrogen/Deuterium Exchange Mass Spectrometry Platform. *Anal. Chem.* **2016,** *88* (12), 6607-6614.

60. Gallagher, E. S.; Hudgens, J. W., Mapping Protein–Ligand Interactions with Proteolytic Fragmentation, Hydrogen/Deuterium Exchange-Mass Spectrometry. *Methods in Enzymology* **2016,** *566*, 357-404.

61. Engen, J. R., Analysis of protein complexes with hydrogen exchange and mass spectrometry. *Analyst* **2003,** *128* (6), 623-628.

62. Engen, J. R.; Wales, T. E., Analytical Aspects of Hydrogen Exchange Mass Spectrometry. In *Annual Review of Analytical Chemistry, Vol 8*, Cooks, R. G.; Pemberton, J. E., Eds. Annual Reviews: Palo Alto, 2015; Vol. 8, pp 127-148.

63. Hamuro, Y.; Coales, S. J., Optimization of Feasibility Stage for Hydrogen/Deuterium Exchange Mass Spectrometry. *J. Am. Soc. Mass Spectrom.* **2018,** *29* (3), 623-629.

64. Marino, J. P.; Brinson, R. G.; Hudgens, J. W.; Ladner, J. E.; Gallagher, D. T.; Gallagher, E. S.; Arbogast, L. W.; Huang, R. Y. C., Emerging Technologies To Assess the Higher Order Structure of Monoclonal Antibodies. In *State-of-the-Art and Emerging Technologies for Therapeutic Monoclonal Antibody Characterization, Vol 3: Defining the Next Generation of Analytical and Biophysical Techniques*, Schiel, J. E.; Davis, D. L.; Borisov, O. V., Eds. 2015; Vol. 1202, pp 17-43.

65. Karageorgos, I.; Gallagher, E. S.; Galvin, C.; Gallagher, D. T.; Hudgens, J. W., Biophysical characterization and structure of the Fab fragment from the NIST reference antibody, RM 8671. *Biologicals* **2017,** *50*, 27-34.

66. Gallagher, D. T.; Karageorgos, I.; Hudgens, J. W.; Galvin, C. V., Data on crystal organization in the structure of the Fab fragment from the NIST reference antibody, RM 8671. *Data in Brief* **2018,** *16*, 29-36.

67. Zhang, H. M.; McLoughlin, S. M.; Frausto, S. D.; Tang, H. L.; Emmettt, M. R.; Marshall, A. G., Simultaneous Reduction and Digestion of Proteins with Disulfide Bonds for Hydrogen/Deuterium Exchange Monitored by Mass Spectrometry. *Anal. Chem.* **2010,** *82* (4), 1450-1454.

68. Bai, Y. W.; Milne, J. S.; Mayne, L.; Englander, S. W., Primary Structure Effects on Peptide Group Hydrogen-Exchange. *Proteins-Structure Function and Genetics* **1993,** *17* (1), 75-86.

69. Cravello, L.; Lascoux, D.; Forest, E., Use of different proteases working in acidic conditions to improve sequence coverage and resolution in hydrogen/deuterium exchange of large proteins. **2003,** *17* (21), 2387-2393.

70. Hamuro, Y.; Zhang, T., High-Resolution HDX-MS of Cytochrome c Using Pepsin/Fungal Protease Type XIII Mixed Bed Column. *J. Am. Soc. Mass Spectrom.* **2019,** *30*, XXX-XXX.

71. Hvidt, A.; Nielsen, S. O., Hydrogen Exchange in Proteins. In *Advances in Protein Chemistry*, Anfinsen, C. B.; Anson, M. L.; Edsall, J. T.; Richards, F. M., Eds. Academic Press: 1966; Vol. 21, pp 287-386.

72. Englander, S. W.; Kallenbach, N. R., Hydrogen-Exchange and Structural Dynamics of Proteins and Nucleic-Acids. *Quarterly Reviews of Biophysics* **1983,** *16* (4), 521-655.

73. Mayne, L., Chapter Thirteen - Hydrogen Exchange Mass Spectrometry. In *Methods in Enzymology*, Kelman, Z., Ed. Academic Press: 2016; Vol. 566, pp 335-356.

74. Hudgens, J. W.; Gallagher, E. S.; Karageorgos, I.; Anderson, K. W.; Huang, R. Y.-C.; Chen, G.; Bou-Assaf, G. M.; Espada, A.; Chalmers, M. J.; Harguindey, E.; Zhang, H.-M.; Walters, B. T.; Zhang, J.; Venable, J.; Steckler, C.; Park, I.; Brock, A.; Lu, X.; Pandey, R.; Chandramohan, A.; Anand, G. S.; Nirudodhi, S. N.; Sperry, J. B.; Rouse, J. C.; Carroll, J. A.; Rand, K. D.; Leurs, U.; Weis, D. D.; Al-Naqshabandi, M. A.; Hageman, T. S.; Deredge, D.; Wintrode, P. L.; Papanastasiou, M.; Lambris, J. D.; Li, S.; Urata, S., Hydrogen-Deuterium Exchange Mass Spectrometry (HDX-MS) Centroid Data Measured between 3.6 °C and 25.4 °C for the Fab Fragment of NISTmAb. *JRes NIST* **2019,** *124*, 124009.

75. Yury, K.; Alexey, K.; Igor, P.; Eugene, N., Conformational changes of ubiquitin during electrospray ionization as determined by in-ESI source H/D exchange combined with high-resolution MS and ECD fragmentation. *Journal of Mass Spectrometry* **2014,** *49* (10), 989-994.

76. Kim, H. J.; Liyanage, O. T.; Mulenos, M. R.; Gallagher, E. S., Mass Spectral Detection of Forward- and Reverse-Hydrogen/Deuterium Exchange Resulting from Residual Solvent Vapors in Electrospray Sources. *J. Am. Soc. Mass Spectrom.* **2018**.

77. Filliben, J. J.; Tobias, P.; Trutna, L., Design of Experiments (DOE) Mean Plot. In *NIST/SEMATECH e-Handbook of Statistical Methods*, National Institute of Atndards and Technology: 2003.

78. Heckert, N. A.; Filliben, J. J. Dataplot. http://www.itl.nist.gov/div898/software/dataplot/ (accessed 4 OCT 2017).

79. Filliben; J., J., "DATAPLOT—Introduction and Overview", NIST Special Publication 667 pdf version. National Bureau of Standards: Gaithersburg, MD, 1984. http://www.itl.nist.gov/div898/software/dataplot/sp667.pdf.

80. Fang, J.; Rand, K. D.; Beuning, P. J.; Engen, J. R., False EX1 signatures caused by sample carryover during HX MS analyses. *International journal of mass spectrometry* **2011,** *302* (1-3), 19-25.

81. Majumdar, R.; Manikwar, P.; Hickey, J. M.; Arora, J.; Middaugh, C. R.; Volkin, D. B.; Weis, D. D., Minimizing Carry-Over in an Online Pepsin Digestion System used for the H/D Exchange Mass Spectrometric Analysis of an IgG1 Monoclonal Antibody. *J. Am. Soc. Mass Spectrom.* **2012,** *23* (12), 2140-2148.

82. Jensen, P. F.; Rand, K. D., Hydrogen Exchange: A Sensitive Analytical Window into Protein Conformation and Dynamics. In *Hydrogen Exchange Mass Spectrometry of Proteins: Fundamentals, Methods, and Applications*, 1st Ed. ed.; Weis, D. D., Ed. John Wiley & Sons, Ltd.: Chichester, 2016; pp 1-17.

83. Zhang, Z.; Fang, J., Extracting Information from Hydrogen Exhange Mass Spectrometry Data In *Hydrogen Exchange Mass Spectrometry of Proteins: Fundamentals, Methods, and Applications*, 1st ed.; Weis, D. D., Ed. John Wiley & Sons, Ltd.: Chichester, 2016; pp 107-125.

84. Zhang, Z.; Smith, D. L., Determination of amide hydrogen exchange by mass spectrometry: A new tool for protein structure elucidation. *Protein Science* **1993,** *2*, 522-531.

85. López-Ferrer, D.; Petritis, K.; Robinson, E. W.; Hixson, K. K.; Tian, Z.; Lee, J. H.; Lee, S.-W.; Tolić, N.; Weitz, K. K.; Belov, M. E.; Smith, R. D.; Paša-Tolić, L., Pressurized Pepsin Digestion in Proteomics: An Automatable Alternative to Trypsin for Integrated Top-Down Bottom-Up Proteomics. *Molecular & Cellular Proteomics : MCP* **2011,** *10* (2), M110.001479.

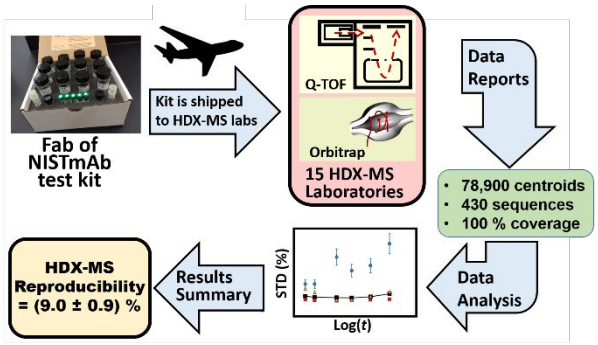

Figure for TOC

86. Ahn, J.; Cao, M.-J.; Yu, Y. Q.; Engen, J. R., Accessing the Reproducibility and Specificity of Pepsin and other Aspartic Proteases. *Biochim Biophys Acta.* **2013,** *1834(6)*, 1222–1229.

87. NIST/SEMATECH e-Handbook of Statistical Methods. https://www.itl.nist.gov/div898/handbook/eda/section3/eda366i.htm (accessed 6/4/2018).

88. Hamuro, Y.; Coales, S. J.; Molnar, K. S.; Tuske, S. J.; Morrow, J. A., Specificity of immobilized porcine pepsin in H/D exchange compatible conditions. *Rapid Commun. Mass Spectrom.* **2008,** *22* (7), 1041-1046.